JMB

Crystal Structure of a Non-canonical Low-affinity Peptide Complexed with MHC Class I: A New Approach For Vaccine Design

Vasso Apostolopoulos[1,2]*, Minmin Yu[1], Adam L. Corper[1], Luc Teyton[3] Geoffrey A. Pietersz[3], Ian F. C. McKenzie[3] and Ian A. Wilson[1,4]*

[1]*Department of Molecular Biology, BCC-206 The Scripps Research Institute 10550 North Torrey Pines Road La Jolla, CA 92037, USA*

[2]*The Austin Research Institute Immunology and Vaccine Laboratory, Studley Road Heidelberg, Vic. 3084 Australia*

[3]*Department of Immunology The Scripps Research Institute 10550 North Torrey Pines Road La Jolla, CA 92037, USA*

[4]*Skaggs Institute for Chemical Biology, The Scripps Research Institute, 10550 North Torrey Pines Road, La Jolla, CA 92037 USA*

Corresponding authors

Peptides bind with high affinity to MHC class I molecules by anchoring certain side-chains (anchors) into specificity pockets in the MHC peptide-binding groove. Peptides that do not contain these canonical anchor residues normally have low affinity, resulting in impaired pMHC stability and loss of immunogenicity. Here, we report the crystal structure at 1.6 Å resolution of an immunogenic, low-affinity peptide from the tumor-associated antigen MUC1, bound to H-2K^b. Stable binding is still achieved despite small, non-canonical residues in the C and F anchor pockets. This MUC1/K^b structure reveals how low-affinity peptides can be utilized in the design of novel peptide-based tumor vaccines. The molecular interactions elucidated in this non-canonical low-affinity peptide MHC complex should help uncover additional immunogenic peptides from primary protein sequences and aid in the design of alternative approaches for T-cell vaccines.

Keywords: tumor peptide; non-canonical anchor motif peptides; MUC1; tumor immunotherapy; H-2K^b

Introduction

Antigen recognition by T-cells is central to the generation and regulation of an effective immune response. The first step in T-cell generation is the uptake and presentation of antigenic peptides by MHC molecules on antigen-presenting cells. Crystallographic studies of MHC class I molecules have revealed that the amino and carboxy termini of high affinity 8–10-mer peptides (P1–Pn) are tethered in the groove by conserved hydrogen bond networks.[1–3] The side-chains of bound peptides differentially occupy various specificity pockets (A–F) that form in the binding groove between the long α1 and α2 helices and the β-sheet platform.[4] By determining the amino acid sequence of peptides eluted from purified class I molecules, each MHC allele was found to have preferences for particular amino acids at (usually) two particular positions (anchors) in the peptide.[5,6] However, this method fails to identify low-affinity peptides that are lost prior to elution.

Anchors for most class I alleles are found at P2 (B pocket) and at the usual C-terminal residue P9 (F pocket). However, H-2K^b binds equally well to canonical 8-mer and 9-mer peptides containing preferred anchors Phe/Tyr for the central P5/6 residues (C pocket), Leu at the C terminus (P8/9) (F pocket), and, in some instances, Tyr at P3 (D pocket). Although these anchor residues are usually necessary for high-affinity binding and stabilization of individual MHC isotypes, the presence of appropriate anchors is not a sufficient prerequisite to define production of high-affinity

(a)

(b)
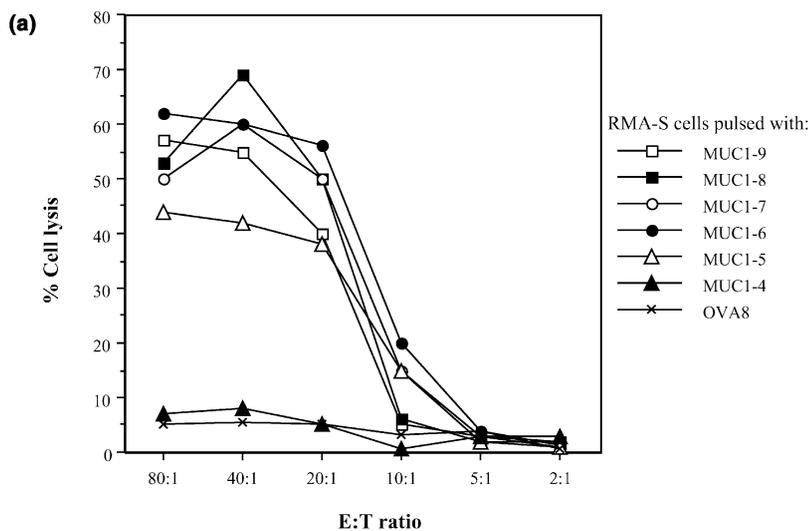
Affinity measurements of peptides binding to H-2K^b

Peptide	Sequence	4°C K$_D$ (nM)	23°C K$_D$ (nM)	37°C K$_D$ (nM)
MUC1-8	SAPDTRPA	433	877	37000
MUC1-8-5F	SAPDFRPA	460	130	4900
MUC1-8-8L	SAPDTRP**L**	150	250	8900
MUC1-8-5F8L	SAPDFRP**L**	160	60	300
MUC1-9	SAPDTRPAP	54150	15900	17100
SEV9	FAPGNYPAL	5	3	30
OVA8	SIINFEKL	6	10	82
VSV8	RGYVYQGL	34	27	163

The affinity values in this table are the means of 5 values.
The standard errors of these values are between 10-15%.

Figure 1. Peptide binding to H-2K^b. (a) CTL assay using MUC1 peptides of different lengths. CTL are derived from spleen cells of C57BL/6 mice immunized with M-FP. Target RMA-S cells were pulsed with varying length peptides as shown and expressed as % specific chromium release (cell lysis) *versus* E:T ratio. This experiment was repeated three times and representative data sets are shown. OVA8 represents a control peptide that binds to H-2K^b. (b) Affinity measurements of various peptides that bind to H-2K^b (see Materials and Methods).

MHC−peptide complexes.[7] Peptide analog studies have demonstrated an important role for secondary anchor positions and substantial improvements in epitope predictions have resulted from the development of more extended motifs that include these additional sequence preferences.[8] Nevertheless, peptides that do not contain canonical anchor motifs, and which usually bind with low affinity, can be presented to CD8$^+$ cytotoxic T lymphocyte (CTL), such that cell lysis occurs.[9−14] However, it has not been clear how such non-standard or low-affinity peptides are presented by MHC class I molecules and, hence, how they can serve as targets for CTL.

Recently, considerable emphasis has been placed on finding tumor-associated antigens that could serve as targets for immunotherapy. MUC1, a high molecular mass glycoprotein, is highly expressed on cancer cells of the breast, pancreas, colon and ovary. MUC1 has a ubiquitous cellular distribution and is aberrantly glycosylated on cancer cells, such that new peptide epitopes emerge. MUC1 contains a repeating motif region (VNTR) of 20 amino acid residues (PDTRPAPGSTAPPAH-GVTSA) that is immunogenic in mice and gives rise to coordinated antibody and CTL responses.[15−17] We have demonstrated that MUC1 VNTR fusion protein when conjugated to oxidized mannan (M-FP), can generate CD8$^+$ MHC-restricted CTLs, at high CTL precursor frequencies, protect mice from challenge with MUC1$^+$ tumors, and lead to reversal of the growth of established MUC1$^+$ tumors.[12−14,17−22] Subsequent studies demonstrated that CTLs could be induced against MUC1 presented by most H-2 and HLA alleles.[12,13] The peptide sequences presented by H-2K^b targets as a 9-mer (SAPDTRPAP; MUC1-9), or an 8-mer (SAPDTRPA; MUC1-8), do not contain the K^b consensus anchor motifs at P5/6 and P8/9, consistent with low-affinity peptide binding.[13]

Table 1. Comparison of standard anchor and non-canonical binding peptides of H-2K^b

Peptide sequence	Source	Reference
1 2 3 4 5 6 7 8		
S A P D T R P A	MUC1 VNTR (MUC1-8)[a]	13
S I I N F E K L	Chicken ovalbumin$_{257-264}$ (OVA8)[a]	60
R G Y V Y Q G L	Vesicular stomatitis virus NP$_{52-59}$ (VSV8)[a]	61
S S I E F A R L	HSV glycoprotein B$_{498-505}$	62
F E Q N T A Q P	Lewis lung Carcinoma (MUT1)	9
F E Q N T A Q A	Lewis lung Carcinoma (MUT2)	9
S I Y R Y Y G L	Synthetic strong agonist for 2C TCR (SIYR)[a]	63
E Q Y K F Y S V	Self agonist for 2C TCR (dEV8)[a]	63
L S P F P F D L	Weak agonist for 2C TCR (p2Ca)	64
R G Y V Y Q E L	Antagonist for 2C TCR (EVSV)	65
1 2 3 4 5 6 7 8 9		
S A P D T R P A P	MUC1 VNTR (MUC1-9)	13
S R D H S R T P M	Yeast (YEA9)[a]	29
F A P G N Y P A L	Sendai virus NP$_{324-332}$ (SEV9)[a]	66
Y S G Y I F R D L	Rotavirus VP3$_{585-593}$	67
R F H N I R G R W	E6, HPV type 16	11

Amino acids given in red are the standard anchor motifs for peptide binding to H-2K^b molecules.[5] Amino acids given in blue are non-optimal side-chains found in peptides associated with H-2K^b molecules. The one-letter code for the amino acids are used. In H-2K^b, the longer 9-mer peptides bulge out between P4 and P6, but the positions of their ends are conserved; hence, the gap introduced between P4 and P5 for 8-mer peptides is to maintain similar alignment in 8-mer and 9-mer peptides.
[a] Crystal structures of these peptide complexes are known (see Figures 2 and 3).

Here, we describe the high-resolution crystal structure of this low-affinity, non-canonical anchor MUC1-8 peptide in association with H-2K^b at 1.6 Å.

Results

Identification of non-canonical peptides binding MHC class I molecules

Immunization of mice with M-FP generates CD8$^+$ CTL that protect mice against an MUC1$^+$ tumor challenge.[18−22] The 9-mer peptide SAPDT-RPAP (MUC1-9) is presented by H-2K^b;[13] 5−8-mers can also be presented by RMA-S target cells (Figure 1(a)), but not the 4-mer, SAPD, indicating that Thr at P5 plays an important role for stability of the MHC−peptide interaction. Short immunogenic peptides that have been identified for other MHC class I include a 4-mer (PFDL) and a 5-mer (HFMPT) for H-2L^d.[23−25] H-2K^b can also bind a MUC1-9 peptide that is extended by up to five residues at the C terminus (V.A. *et al.*, unpublished results), similar to the VSV8 peptide, where four residues could be added at the C terminus, but not at the N terminus.[26] A crystal structure of a 10-mer peptide bound to HLA-A2 showed that a single residue extension at the C terminus projected out of the binding groove.[27] Furthermore, we previously demonstrated that MUC1-9 could loop out sufficiently at the C terminus, when complexed to H-2K^b, to be detected by anti-MUC1 peptide monoclonal antibodies.[14]

The amino acid sequences for MUC1-8 (SAPD-TRPA) and MUC1-9 (SAPDTRPAP) do not contain either Phe/Tyr at P5/6 or Leu at P8/9 that are usually associated with high-affinity binding to H-2K^b.[5,6] MUC1-8 has small non-polar Ala residues at P2 and P8 and a small polar Thr residue at P5

Table 2. Crystallographic data collection and refinement statistics

Cell dimensions (Å)	$a = 136.1$, $b = 89.4$, $c = 45.3$
R_{sym} (%)[a]	3.1 (51.5)[b]
Resolution range (Å)	50.0–1.6
Unique reflections	68,318 (3254)
$\langle I/\sigma \rangle$	32.8 (2.3)
Data redundancy	3.7 (3.1)
Data completeness (%)	92.3 (88.1)
R_{cryst} (%)[c]	21.2
R_{free} (%)[d]	22.1
Bond length rmsd (Å)	0.005
Bond angle rmsd (deg.)	1.33
Average B-values (Å^2) (Protein (peptide))	27 (33)
No. water molecules (average B in Å^2)	235 (33)
Ramachandran plot analysis[e]	
Residues in most favored regions (%)	92.1
Residues in additional allowed regions (%)	7.6
Residues in generously allowed regions (%)	0.3
Residues in disallowed regions (%)	0.0

[a] $R_{sym} = 100[\Sigma_h \Sigma_i |I_i(h) - \langle I(h) \rangle| / \Sigma_h \Sigma_i I_i(h)]$, where $I_i(h)$ is the ith observation of the intensity of reflection h and $\langle I(h) \rangle$ is the mean value of all $I(h)_i$.
[b] Data for the highest-resolution shell, 1.63–1.60 Å.
[c] $R_{cryst} = \Sigma||F_o| - |F_c||/\Sigma|F_o|$, where F_o and F_c are the observed and calculated structure factor amplitudes within the set of reflections used for refinement.
[d] $R_{free} = \Sigma||F_o| - |F_c||/\Sigma|F_o|$ was calculated for a randomly selected set of structure factors ($\sim$10%) and not used in refinement.
[e] The Ramachandran plot was generated using PROCHECK.[59]

(Table 1). Other H-2K^b "anchorless" peptides for which specific CTLs have been generated include MUT1 (FEQNTAQP), and MUT2 (FEQNTAQA), isolated from Lewis lung carcinoma,[9] and the tumor-associated E6 human papillomavirus type-16 protein (RFHNIRGRW)[11] (Table 1). Thus, it was of significant interest that CTL could be generated against MUC1 presumably due to a compensatory high-affinity recognition of TCR for the MHC–MUC1 peptide complex (although this cannot be resolved until the crystal structure of a TCR–peptide–MHC class I complex with MUC1-8 peptide is determined).[13] Exhaustive efforts to crystallize the H-2K^b/MUC1-9 complex failed, presumably due to its even lower-affinity interaction with H-2K^b. Thus, we proceeded with the crystal structure determination of H-2K^b/MUC1-8 complex which, although of higher affinity (by 100-fold) than MUC1-9, is at least 100-fold lower than most high-affinity H-2K^b binding peptides (Table 1, Figure 1(b)).

We determined the crystal structure of H-2K^b/MUC1-8 to elucidate how low-affinity, non-canonical anchored peptides bind to MHC class I molecule and how relatively weak interactions can stabilize the peptide–MHC sufficiently for recognition by CTL. This H-2K^b/MUC1-8 structure was compared to high-affinity, canonical peptides OVA8 and VSV8.

Affinity measurements of non-canonical peptide (MUC1-8) with H-2K^b

Affinity and stabilization experiments with the OVA8 peptide have demonstrated that P2/3, P5 and P8 are important for H-2K^b binding, while P4, P6 and P7 affect CTL recognition.[28] In that study, the Ile-P2/Phe-P5 combination had the highest affinity for H-2K^b followed by (in decreasing

order) Val-P2/Phe-P5, Ala-P2/Phe-P5, Asn-P2/Tyr-P5, Phe-P2/Phe-P5 and Glu-P2/Tyr-P5. However, secondary anchors, such as P3, can affect this order. As the MUC1-8 peptide does not contain any preferred anchor residues at P2, P5 and P8, it was likely to bind with low affinity. Indeed, affinity measurements failed to detect binding by immunoprecipitation.[13] However, the affinity of MUC1-8 measured in an inhibition assay was 4.3×10^{-7} M at 4 °C, 8.7×10^{-7} M at 23 °C (100–300-fold lower than OVA8, VSV8 or SEV9, Figure 1(b)), but at 37 °C MUC1-8 provided little thermal stabilization to H-2K^b (3.7×10^{-5} M; 500–1000-fold lower than OVA8 or VSV8 or SEV9, Figure 1(b)). Mutation of Thr-P5 to Phe-P5 increased the affinity by about sevenfold at 23 °C and 37 °C; mutation of Ala-P8 to Leu-P8 increased the affinity by about threefold at 23 °C and 37 °C; double mutations of Thr-P5/Ala-P8 to Phe-P5/Leu-P8 increased the affinity even further to 14-fold at 23 °C and provided higher thermal stabilization at 37 °C (Figure 1(b)).

Crystal structure of the H-2K^b–MUC1-8 complex

The crystal structure of H-2K^b–MUC1-8 at 1.6 Å resolution was determined by molecular replacement to an R_{free} value of 22.1% (Table 2). The final model consisted of H-2K^b heavy chain: α1–274, β$_2$-microglobulin: β1–99, four carbohydrate moieties (three at Asnα176 and one at Asnα86) and all peptide residues, P1–P8 (MUC1-8). Electron density for the bound peptide was continuous and well resolved, except for the electron density corresponding to the hydroxyl group of Thr-P5 which was weak (Figure 2(a) and (b)). Furthermore, the B-values for this residue were
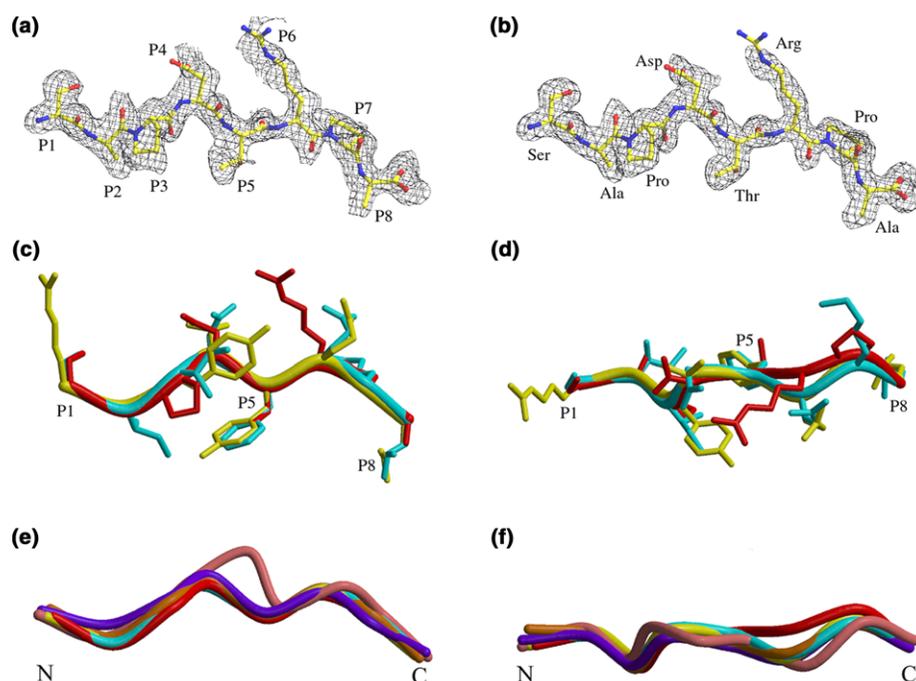
Figure 2. Peptide density and conformation when bound to H-2K^b. (a) and (b) Electron density of the MUC1-8 peptide in the H-2K^b binding groove. (a) Initial $F_o - F_c$ map contoured at 1.5σ prior to any peptide fitting. (b) Final σ$_A$-weighted $2F_o - F_c$ map contoured at 1.0σ for the refined structure at 1.6 Å. (c)–(f) Structure comparisons of selected H-2K^b-bound peptides. Comparison of 8-mer peptides, (c) side view, (d) top view. C^α trace of all known peptides from multiple crystal structures with H-2K^b;[2,29,33,37] peptides are viewed from (e) the side or (f) above looking directly down into the MHC binding groove. H-2K^b residues in the various complexes were superimposed only on their β-sheet floors and the resulting peptide overlaps were produced. The peptide conformations represent their structures in the H-2K^b bound form. Peptides MUC1-8, OVA8, VSV8, dEV8 and SIYR are 8-mers and SEV9 is a 9-mer; the extra residue in SEV9 causes a bulk in the backbone in order to accommodate the same anchors at the N and C terminus.[2] The Figure was drawn using programs MOLSCRIPT and Raster3D. Peptide colors are as follows: MUC1-8, red; OVA8, turquoise; VSV8, yellow; SEV9, salmon; dEV8, purple and SIYR, orange.

high, which is unusual for a side-chain corresponding to a primary anchor position.

Superposition of the β-sheet floor of the H-2K^b α1/α2 domain of MUC1-8, VSV8 and OVA8 shows similar overlays when viewed from the side (Figure 2(c) and (e)); however, significant differences are apparent when viewed from above

Table 3. Comparison of peptide–MHC (H-2K^b) buried surface areas (Å^2)

Peptide	Exposed peptide[a]	Buried peptide[a]	Buried MHC[b]
SEV9	209 (26)	603 (74)	802
dEV8	183 (20)	700 (80)	867
MUC1-8	177 (25)	532 (75)	716
SIYR	174 (20)	689 (80)	839
OVA8	150 (18)	695 (82)	842
VSV8	146 (18)	679 (82)	843

Neighboring molecules in the crystal structures are not included in the calculations. Buried is defined as the molecular surface area inaccessible to a 1.4 Å radius probe when the peptide–MHC complex is formed. Exposed is the molecular surface area accessible to the same probe. Buried surfaces were calculated with MS.[68]
[a] The number in parentheses is the percentage of the total peptide molecular surface area.
[b] Ranked by decreasing exposed peptide.

(Figure 2(d) and (f)). MUC1-8 and VSV8 complexes when superimposed gave average root-mean-square deviations (rmsd) for the peptide C^α positions of 0.57 Å for P1–P4 and 0.93 Å for P5–P8, comparable to rmsd values for other high-affinity H-2K^b complexes (OVA8, dEV8, SIYR). By comparison, superposition of high-affinity peptides, VSV8 and OVA8, gave rmsd values of 0.49 Å for P1–P4 and 0.29 Å for P5–P8. Thus, the largest deviations in MUC1-8 compared to the high-affinity peptides occur between P5 and P8. Significant sidewards displacements of the MUC1-8 peptide backbone towards the α1 helix begin at P5 and reach a maximum at P6 C^α (1.3 Å and 1.7 Å from OVA8 and VSV8, respectively) before converging at P8 (Figure 2(d) and (f)).

A striking feature of MUC1-8 *versus* high-affinity 8-mer peptides is the different extent to which the peptides are buried in the binding groove (Table 3). A total of 532 Å^2 (75%) of the MUC1-8 solvent-accessible surface is buried, whereas 716 Å^2 of H-2K^b becomes inaccessible upon peptide binding. In comparison, for high-affinity 8-mers (OVA8, VSV8, SIYR and dEV8), 679–700 Å^2 (80–82%) of peptide surface area becomes inaccessible to solvent, whereas 839–867 Å^2 of H-2K^b is buried (Table 3). These differences can primarily be
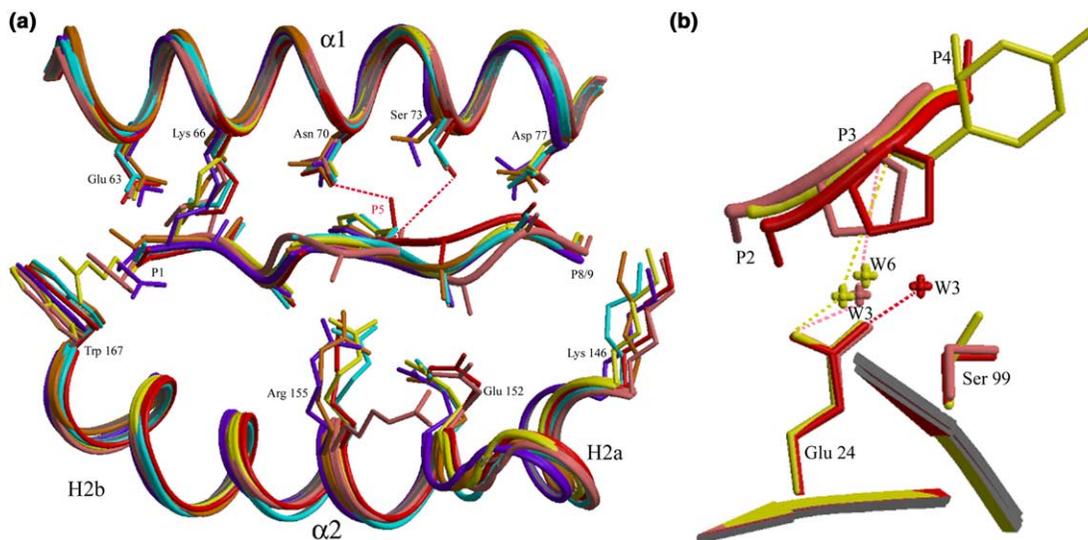
Figure 3. Comparison of the peptide-binding grooves in H-2K^b crystal structures. (a) Six structures were overlapped by superimposition of the β-sheet floor. The α1α2 helices superimpose closely, with some side-chain variations at Lysα66, Asnα70, Serα73, Aspα77, Lysα146, Gluα152, Argα155 and Trpα167. Peptides are shown as C^{α}C^β trace. Novel hydrogen bonds not present in other structures are shown for MUC1-8 (red). (b) Side view of MUC1-8, SEV9 and VSV8 peptides showing P2 and P3 side-chains and P4 C^{α}C^β. The side-chain rotamer differences for Serα99 (MUC1-8/SEV9 compared to VSV8) are shown as well as water molecules (W) forming hydrogen bonds with peptide and/or MHC side-chains in the B–C pocket. The Figure was generated using programs MOLSCRIPT and Raster3D. Peptide colors are as follows: MUC1-8, red; OVA8, turquoise; VSV8, yellow; SEV9, salmon; dEV8, purple and SIYR, orange.

attributed to the small P5 anchor in MUC1-8 and the P5–P8 backbone deviation towards the α1 helix (Figure 2).

Interactions of the low-affinity non-canonical MUC1-8 peptide with H-2K^b

The interactions and conformation of MUC1-8 with H-2K^b exhibit many of the key principles gleaned from crystal structures with high-affinity binding peptides, VSV8, OVA8 and SEV9.[1,3,29] High-affinity interactions are consistent with the formation of a highly conserved hydrogen bond network between side-chains of the MHC and the peptide backbone, mainly around the N and C termini, and the optimal fit of peptide side-chains into the anchor pockets. It was not clear prior to their structure determination whether the relatively low affinity of non-canonical anchor peptides would be due to loss of main-chain hydrogen bonds at the termini or of non-optimal occupation of anchor pockets. Our structural analysis indicates that the number of hydrogen bonds to the peptide backbone for the low-affinity MUC1-8 peptide is, in fact, almost identical with the high-affinity complexes. Furthermore, the hydroxyl group of Thr-P5 in MUC1-8 makes a novel hydrogen bond with Asnα70 O^{δ1} (Figure 3(a)). In addition, a hydrogen bond between Serα73 O^γ and the main-chain amide group at P5 is present in MUC1-8 (as well as VSV8 and SEV9), but not in OVA8 (Figure 3(a)). Thus, somewhat surprisingly, all of the main-chain hydrogen bonds are maintained in the MUC1-8 complex. Nine water-mediated hydrogen bonds are found

in the MUC1-8 complex compared to ten in OVA8 and 11 in SEV9. More surprisingly, all of the water-mediated hydrogen bond interactions in MUC1-8 complexes are present in one or other of the OVA8, VSV8 or SEV9 complexes.

Peptide stability and high affinity are also dependent on optimally filling the pockets in the core of the binding groove.[3,4] While different length peptides can be accommodated by bulging out in the center of the groove,[2,30] specific anchor residues are usually required for optimal stability. The OVA8 peptide has large non-polar residues at P2 and at P5 which enable an extremely tight hydrophobic packing in the inter-connected P2–P5 pockets, whereas VSV8 has Gly-P2 and Tyr-P5 and contains a large secondary anchor at Tyr-P3. Similarly, SEV9 has one large side-chain, Tyr-P6 and a small Ala-P2, but with a Pro-P3, which helps close the B–C pockets. In the latter two structures, solvent molecules help fill up the B–C pocket and mediate hydrogen bond contacts with hydrophilic residues (Gluα24, Serα99), which are buried on the β-sheet floor (Figure 4). A conserved water molecule (designated for comparative reasons as W1; Figure 4) is present in all structures.

Comparison of the relative filling or occupancy of the H-2K^b B and C specificity pockets by MUC1-8, OVA8 and VSV8 reveals major differences. MUC1-8 has small side-chains at P2, P5 and P8 and a buried water molecule (W2) that only partially compensates in filling the B–C space (Figure 4). In contrast, OVA8 has a bulky Ile at P2 that packs tightly into the B pocket adjacent to Phe-P5 (C pocket) leaving no space for water. Indeed, replacement of the OVA8 Phe-P5 with
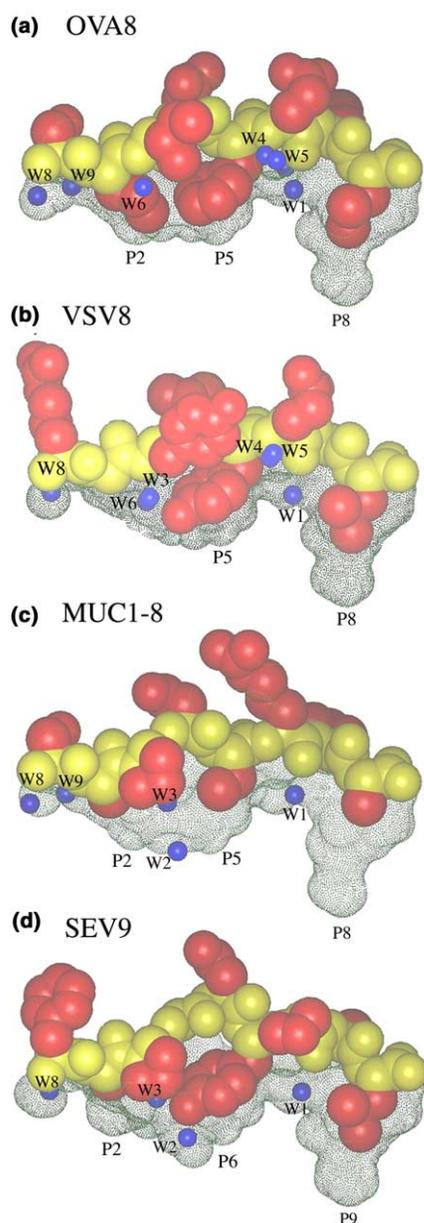
(a) OVA8

(b) VSV8

(c) MUC1-8

(d) SEV9

Figure 4. Comparison of occupancy of specificity pockets in different H-2K^b structures. (a) OVA8, (b) VSV8, (c) MUC1-8 and (d) SEV9. Molecular surfaces for the MHC-binding groove (dotted surface) were calculated with a probe radius of 1.4 Å with Insight II (Biosym Technologies, San Diego CA, USA). The peptides are in CPK space-filling representation (backbone, yellow; side-chains, red) and labelled P1–P8 or P1–P9. P2 occupies the B pocket, P5/6 the C pocket and P8/9 the F pocket. Water molecules (W) rendered as spheres of one-half van der Waals radii are colored blue.

Tyr significantly decreases the stability of the complex.[31] W3, in SEV9 and VSV8, forms a hydrogen bond between the carbonyl oxygen atom of P3 and Gluα24; however, in MUC1-8, W3 is shifted (1.7 Å) to reduce the size of the B–C cavity (NB: the *B*-value is high for this water molecule relative to other buried water molecules in the same structure) and forms a hydrogen bond only to Gluα24.

Most significantly, W4 and W5 in OVA8 and VSV8 are absent in MUC1-8 and SEV9, forming a cavity in MUC1-8, but not in SEV9, due to the presence of Pro-P7 (Figures 4 and 5). W6, is displaced by Pro-P3 in SEV9 and MUC1-8 and, as a result, an alternate rotamer of Serα99 shifts the hydroxyl group by 2.0 Å in SEV9 (salmon) and MUC1-8 (red) compared to VSV8 (yellow) (Figure 3(b)). W8 is conserved in all the structures and W9 is present in OVA8 and MUC1-8. The P8/9 pocket is only moderately filled with Leu in OVA8, SEV9 and VSV8 (Figure 4); however, MUC1-8 has a much smaller Ala residue, which leaves the P8 pocket essentially empty, and, surprisingly, no ordered water molecules are found there.

It has been previously noted that peptide-specific differences are induced in MHC side-chain conformations for the OVA8, VSV8 and SEV9 complexes at residues Gluα63, Lysα66, Asnα70, Serα73, Aspα77, Lysα146, Gluα152, Argα155 and Trpα167.[2,29] Some of the same conformational variations occur in the MUC1-8 crystal structure (Figure 3(a)), but no obvious correlations arise between high and low-affinity peptides and conformational changes in the MHC. Thus, conformational changes in H-2K^b reflect the accommodation of the different bound peptide sequences and not changes in the affinity or stability of the peptide. Similar observations have been reported for five HLA-A2 peptide complexes at Argα97, Tyrα116 and Trpα167.[32] However, the transmission of peptide-induced conformational changes to the MHC can enhance the discrimination of individual peptide–MHC complexes by the T-cell receptor, as proposed from the original analysis of the SEV9 and VSV8 complexes,[2] particularly when the altered residues are key TCR contact residues, such as Arg155.[33]

In summary, the low-affinity non-canonical MUC1-8 peptide binds with the same overall features to MHC class I, as all peptides (low or high-affinity) start and finish at the same N and C termini locations; however, deviations occur within the central region of the peptide. The small peptide anchoring side-chains at P2, P5 and P8 of MUC1-8 make use of the canonical B, C and F pockets, respectively. However, the absence of water molecules between the C and E pockets and the large cavity at the side of the C pocket (see below), appear then to contribute most to the low affinity and stability of MUC1-8 with H-2K^b.

Cavities and side-chain flexibility in the P5 ("C") pocket

Internal cavities have been associated with increased conformational flexibility and multiple side-chain conformations for a single protein.[34] A large cavity (139 Å^3) is present for MUC1-8 at the side of the C pocket, as a result of the poor fit and small side-chain at P5 (Figure 5). This cavity extends between the side-chain of Thr-P5 and the H2a and H2b helices of the α2-domain, close to
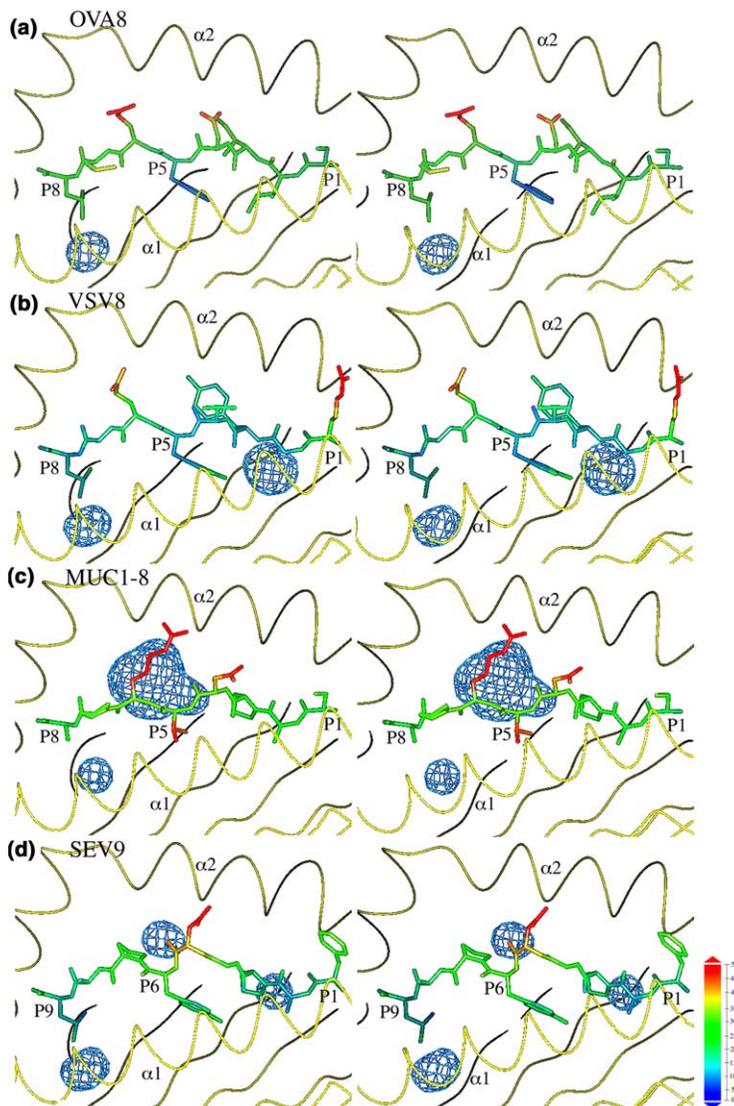
Figure 5. Stereo views of internal cavities formed between the peptide and H-2K^b. (a) OVA8, (b) VSV8, (c) MUC1-8 and (d) SEV9. The peptide trace is represented by their *B*-values (blue ∼5 Å^2 to red ∼48 Å^2) and are oriented from P8/9 (left) to P1 (right). Figure generated with Insight II. Internal cavities (blue mesh) were calculated using the program SURFNET[68] in the presence of bound water. A large internal cavity is found in the non-canonical peptide complex, MUC1-8, compared to the standard high-affinity peptide complexes (OVA8, VSV8, SEV9).

the same region where the maximum backbone deviation of the MUC1-8 peptide occurs and where the W4/W5 water molecules are absent; this cavity is not present in the high-affinity 8-mer or 9-mer MHC−peptide complexes, VSV8, OVA8 or SEV9 (Figure 5). Cavities at this main central anchor position would be expected to decrease substantially the binding affinity of the peptide, as seen with MUC1-8.

While it is difficult to estimate stability accurately, studies on the stability of native conformations of folded proteins suggest that the free energy increases by 24–33 cal M^{-1} per Å^3 of cavity volume (1 cal = 4.184 J).[35] Thus, the cavity at the C pocket in MUC1-8 would be expected to reduce the stability by 3.7–4.6 kcal M^{-1}. Three different peptides binding to H-2K^b and five different peptides to HLA-A2 have been found to have binding free energy differences between 4.4 and 5.2 kcal M^{-1}.[36] Thus, a loss of 3.7–4.6 kcal M^{-1} in MUC1-8 binding to MHC would be expected to decrease substantially the binding affinity and

stability of the peptide. Large cavities are also present in the interfaces of weak affinity peptide−MHC−TCR complexes.[33,37,38]

A small cavity (14–26 Å^3) is present in the F pocket for all complexes (high and low-affinity). Surprisingly, the different side-chain lengths at P8/9 (Leu, Ala) do not seem to play a major role in the cavity size (presumably due to slight adjustments in the protein), or in the affinity of peptides, especially of 9-mer peptides. This situation is consistent with other studies addressing the role of the P8/9 anchor in the affinity or stabilization of peptides bound to H-2K^b.[3,39,40] High-affinity peptides, VSV8 and SEV9, have in addition only a very small cavity (16 Å^3 and 39 Å^3, respectively) at the B pocket, whereas OVA8 is almost a perfect fit for all buried pockets other than F.

The importance of such cavities for the stability of the peptide binding to H-2K^b is exemplified when the *B*-values of the individual residues are examined (Figure 5). The *B*-value is a measurement of the average displacement of an atom due to
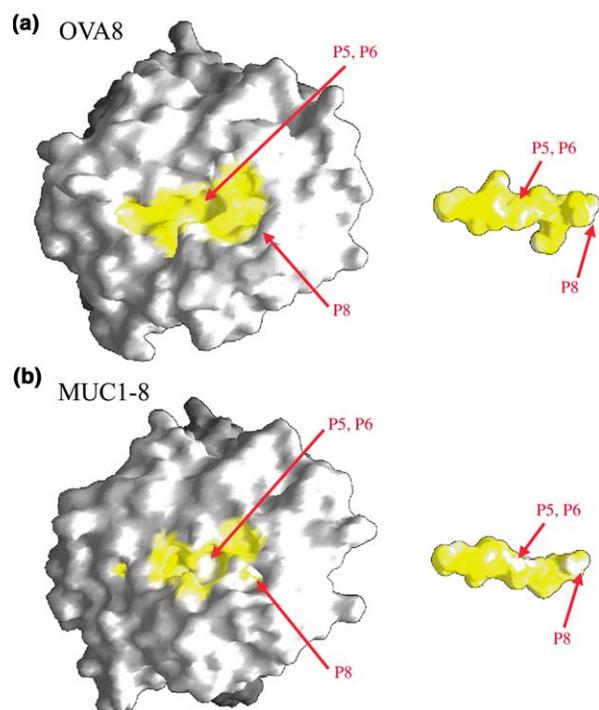
(a) OVA8

(b) MUC1-8

Figure 6. Surface complementarity at the peptide−MHC interface. For calculations of surface complementarity coefficients, the program MS[44] and SPACE[41] were used with a radius sphere of 1.7 Å, a distance cut-off of 5 Å, and a bandwidth for excluding the perimeter of 1.5 Å. The left side shows the molecular surface of MHC (viewed from above) and the right side shows the molecular surface of the peptide (viewed from below). (a) OVA8, and (b) MUC1-8. The molecular surface is colored according to surface complementarity with higher surface complementarity values corresponding to yellow areas and weaker values corresponding to white. Peptide residues P5 and P8 are labeled. The Figure was produced with GRASP.[69]

thermal motion, conformational disorder, and static lattice disorder. The highest *B*-values in the peptide are usually observed for upward-pointing residues (P4/P6, 8-mers and P5/P7, 9-mers; >40 Å²) (Figure 5). The side-chains pointing down into the MHC groove generally have low *B*-values, suggestive of a tight fit, as observed for the side-chains of high-affinity peptides, OVA8, VSV8, dEV8, SIYR (at P2/5/8) and SEV9 (P2/6/9) (9−25 Å²) (Figure 5). However, MUC1-8 has a relatively high *B*-value at Thr-P5 (45 Å²), indicative of a non-optimal local fit, and possible flexibility in the P5/6 pocket. However, the *B*-values for the equivalent MHC side-chains in the P5/P6 pocket are low, whereas the water molecule (W3) in MUC1-8 has a high *B*-value (45 Å²), again indicating that W3 and Thr-P5 for MUC1-8 are not optimal and may have some flexibility within the C pocket. The low *B*-values at P2 and P8 (14−28 Å²), for both low and high-affinity peptides, indicate that these side-chains bind tightly to the B and F pockets, respectively.

Thus, it appears that there is a direct correlation between non-canonical peptide binding with respect to the presence of large cavities within or around the C pocket and high *B*-values for peptide anchors at P5/6. Optimal peptide binding to H-2K^b is critically dependent upon filling the C pocket, which is not the case with MUC1-8.

Shape complementarity in the peptide−MHC interface

Shape complementarity (sc) measures the correlation/match in curvature between two interacting protein surfaces[41] and is used as a structural measure of relative affinity,[42,43] high sc often correlates with affinity, although this is not absolute. Such an analysis of the molecular surface of H-2K^b molecules and bound peptides underlines how OVA8 and VSV8 achieve a slightly better surface sc compared to MUC1-8. The sc parameters in the presence of solvent were calculated to be 0.74 for MUC1, 0.79 for OVA8 and 0.77 for VSV8.[41,44] It is clear from Figure 6 that MUC1-8 has low sc around its central C pocket as compared to OVA8.

Discussion

The mode of binding of high-affinity peptides to murine MHC class I H-2K^b has been described for VSV8, OVA8 and SEV9 peptides.[2,29] However, until now little structural information has been available on the binding of non-standard or low-affinity peptides to MHC class I, and whether they differ substantially in their interaction with MHC molecules and, with the T-cell receptor. It is now apparent from a number of studies that non-standard 8-mer to 9-mer peptides can bind to MHC class I with low affinity, and still be viable targets for CTL.[9−14] We have, therefore, determined the crystal structure of a MUC1-8 peptide lacking the canonical Phe/Tyr-P5 and Leu-P8 anchor sequences, in complex with H-2K^b, and compared its mode of binding to those of standard high-affinity peptides.

We previously reported that antigenic MUC1 peptides, which lacked canonical anchors, could bind to MHC class I (H-2D^b, H-2K^b and HLA-A2), and were still recognized by CTL; they also protected mice against a MUC1$^+$ tumor challenge.[12−14,17−22] A novel mode of binding was suggested, where the N terminus of MUC1-9 was buried, the middle portion arched upward and the C terminus was free such that it could react with anti-peptide antibodies.[14] As MUC1-9 binds with a much lower affinity, it was predicted to have more exposure for antibody interaction. The crystal structure of MUC1-8 in complex with H-2K^b shows that MUC1-8 peptide is clearly less buried in the MHC (by ~150 Å²) than high-affinity binding peptides. However, it is unlikely that even the C terminus of MUC1-8 would be sufficiently exposed for antibody binding. Thus, some other

differences must arise at the C terminus when the longer MUC1-9 peptide is bound.

It might be expected that low-affinity, and/or non-anchor motif peptide structures would have some additional water molecules to help occupy vacated or non-optimally filled pockets. MUC1-8 has no additional water molecules; in fact, two water molecules (W4, W5) are absent, leaving a large cavity at the side of the C pocket. The absence of "rescuing" water molecules[45] to bridge peptide and MHC likely contributes to the low stability and affinity of MUC1-8. Compensatory water molecules have been found in the HLA-A2 complex with an 8-mer peptide (Tax8), after deletion of the P1 residue of Tax9, to help mediate the conserved network of hydrogen bonds at the N terminus of the peptide-binding groove.[46] In addition, the glycopeptide K2G in complex with H-2D^b does not have the consensus Asn-P5 anchor, but instead Ser-O-GlcNAc and, as a consequence, the glycosylated side-chain points upward away from the peptide-binding groove.[47] This substitution leaves the C pocket in the H-2D^b peptide-binding groove empty and hydrogen bonds that are usually formed with the Asn anchor side-chain are instead made with two water molecules.[47] Furthermore, HLA-B53 relative to other alleles has a significant widened peptide-binding groove around the α1 helix, and the presence of additional water molecules enables high-affinity binding of multiple peptide epitopes.[48] In contrast, the large internal cavities present around the C pocket and the high B-value of Thr-P5 in MUC1-8 indicate that peptide side-chain motion is highly likely. Thus, low affinity and stability of peptides in H-2K^b is determined primarily by the direct occupancy of the C pocket and the side-chain residues at P2, P5 and P8. Shape complementarity often correlates with affinity, and small differences were noted between MUC1-8 and OVA8 (Figure 6).

Synthetic peptides are of considerable interest for vaccines and immunotherapy. Efforts to date have been focused mainly on utilizing motifs of high-affinity peptides, as they induce high-avidity CTL. However, most tumor antigens are tumor-associated, in that they are also expressed on normal tissues and overexpressed on tumor cells. Thus, the CTL repertoire of high-affinity peptides would most likely be deleted, but not that for low-affinity epitopes. Hence, it may be more appropriate to use low-affinity binding peptides for immunization. Therefore, low-affinity or non-canonical peptides, which cannot be detected by elution studies and prediction algorithms, could be of equal or greater interest for vaccine programs. Peptide identification by systematic binding studies and CTL assay is possible for major tumor antigens. Mutations could then be made to buried, non-TCR contact amino acid residues of peptides at the normal anchor positions to enhance their affinity for tumor immunotherapy, since the stability of the peptide−MHC complex usually correlates with overall immunogenicity. Indeed, low-affinity MUC1 peptides that bind to HLA-A2 have already been converted by mutation to high-affinity peptides and are currently in a clinical trial (V.A. *et al.*, unpublished results). Furthermore, the H-2K^b low-affinity peptide, MUT1 (a peptide from Lewis lung carcinoma), when mutated at P3, P5 and P8, has increased stability and affinity for RMA-S cells.[49]

Materials and Methods

Mice, immunizations, cytotoxic T lymphocyte assay and peptides

C57BL/6 mice were bred at the Austin Hospital Biomedical Research Laboratory. Mice were immunized intraperitoneally with M-FP weekly for three weeks. Spleen cells from mice immunized with M-FP were obtained seven days after the third immunization and used in a ^{51}Cr release assay as described.[12,13,18,19] The C57BL/6 TAP-deficient cell line, RMA-S, was used as the target cell, which was pulsed with MUC1 peptides at 20 μM. All experiments were repeated at least three times. Shorter peptides are indicative that shorter MUC1 peptides can be presented and recognized by CTL. In this study, the crystal structure of the MUC1-8–MHC complex demonstrates binding of a relatively low-affinity peptide to MHC class I H-2K^b.

SAPDTRPAP, MUC1 VNTR, (MUC1-9); SAPDTRPA, MUC1 VNTR (MUC1-8); SAPDFRPA, (MUC1-8-5F); SAPDTRPL, (MUC1-8-8L); SAPDFRPL, (MUC1-8-5F8L); SAPDTRP, (MUC1-7); SAPDTR, (MUC1-6); SAPDT, (MUC1-5); SAPD, (MUC1-4); FAPGNYPAL, Sendai virus NP$_{324−332}$ (SEV9); SIINFEKL, chicken ovalbumin$_{257−264}$ (OVA8); RGYVYQGL, vesicular stomatitis virus NP$_{52−59}$ (VSV8), were synthesized at the Austin Research Institute, using an Applied Biosystems model 430A machine. The purity of the peptides (>95%) was determined by mass spectrometry.

Affinity measurements of peptides bound to H-2K^b molecules

Affinity measurements for binding of peptides to soluble K^b molecules were performed as described.[50,51] Briefly, VSV8 peptide was labeled with ^{125}I (Amersham Pharmacia Biotech, Buckinghamshire, UK) using the Iodogen method. The [^{125}I]VSV8 peptide was purified using a Sep-Pak column (Waters, Milford, MA). The specific activity of the peptide was 26636 cpm/ng. The competition assays were performed at 4 °C, 23 °C and at 37 °C as described[50] with a few modifications. The binding studies were carried out in 1% (v/v) fetal calf serum (FCS) and the free peptide was removed by gel-filtration on Sephadex columns (NAP-5, Amersham Pharmacia Biotech). The dissociation constants for unlabelled peptides were determined from the molar concentrations of unlabelled peptides that gave 50% inhibition of [^{125}I]VSV8 binding to K^b molecules.

Preparation and crystallization of H-2K^b/MUC1-8 complex

The soluble extracellular domains of H-2K^b (heavy chain residues α1−274 and β$_2$-microglobulin residues

β1–99) were expressed in *Drosophila melanogaster* cells, as described.[2,50–52] Large crystals of the H-2K^b–MUC1-8 complex (10 mg/ml) were grown in 1.8 M NaH$_2$PO$_4$/ K$_2$HPO$_4$ with 2% (v/v) 2-methyl-2,4-pentanediol (MPD), pH 7.25, at 22.5 °C with 100–200-fold molar excess of MUC1-8 peptide.

Data collection and structure determination

Prior to data collection, crystals were harvested for one minute in 1.8 M NaH$_2$PO$_4$/K$_2$HPO$_4$ (pH 7.25), 2% MPD, 1% glycerol followed by a five second soak in mother liquor containing 20% glycerol as cryoprotectant. Crystals were cryocooled to −170 °C in a nitrogen gas stream. X-ray diffraction data were collected at beamline 9-1 of the Stanford Synchrotron Radiation Laboratory (SSRL) on a 345 mm MAR Research imaging plate using a monochromatic wavelength of 1.025 Å. Images were integrated and scaled with DENZO and SCALEPACK.[53] The H-2K^b–MUC1-8 crystals belong to orthorhombic space group $P2_12_12_1$, as do the VSV8 and SEV9 H-2K^b complexes.[2] The structure was determined by molecular replacement using the high-resolution (1.7 Å) H-2K^b– dEV8 (Protein Data Bank (PDB) code 2CKB) by itself (not the H-2K^b–dEV8 complex with TCR)[33] as a search model with the program AMoRe in CCP4.[54] The complex was refined with CNS,[55] by iterative cycles of torsional refinement dynamics, slow-cooling temperature protocols and manual model adjustment. The model was rebuilt from shake-omit maps[34] and σ_A-weighted $2F_o − F_c$ and $F_o − F_c$ maps[56] using the program O.[57] Progress of the refinement was assessed by R_{free} and by avoiding divergence between R_{cryst} and R_{free}.[58] Analysis of the final model with PROCHECK[59] showed 92.1% of the residues are in the most favored regions of the Ramachandran plot, with none in disallowed regions.

Protein Data Bank accession code

The coordinates and structure factors for H-2K^b– MUC1-8 have been deposited in the RCSB Protein Data Bank with accession code 1G7Q.

References

1. Madden, D. R., Gorga, J. C., Strominger, J. L. & Wiley, D. C. (1992). The three-dimensional structure of HLA-B27 at 2.1 Å resolution suggests a general mechanism for tight peptide binding to MHC. *Cell*, **70**, 1035–1048.

2. Fremont, D. H., Matsumura, M., Stura, E. A., Peterson, P. A. & Wilson, I. A. (1992). Crystal structures of two viral peptides in complex with murine MHC class I H-2K^b. *Science*, **257**, 919–927.

3. Matsumura, M., Fremont, D. H., Peterson, P. A. & Wilson, I. A. (1992). Emerging principles for the recognition of peptide antigens by MHC class I molecules. *Science*, **257**, 927–934.

4. Saper, M. A., Bjorkman, P. J. & Wiley, D. C. (1991). Refined structure of the human histocompatibility antigen HLA-A2 at 2.6 Å resolution. *J. Mol. Biol.* **219**, 277–319.

5. Rammensee, H. G., Friede, T. & Stevanovic, S. (1995). MHC ligand and peptide motifs: first listing. *Immunogenetics*, **41**, 178–228.

6. Falk, K., Rotzschke, O., Stevanovic, S., Jung, G. & Rammensee, H. G. (1991). Allele-specific motifs revealed by sequencing of self-peptides eluted from MHC molecules. *Nature*, **351**, 290–296.

7. Ruppert, J., Sidney, J., Celis, E., Kubo, R. T., Grey, H. M. & Sette, A. (1993). Prominent role of secondary anchor residues in peptide binding to HLA-A2.1 molecules. *Cell*, **74**, 929–937.

8. Kast, W. M., Brandt, R. M., Sidney, J., Drijfhout, J. W., Kubo, R. T., Grey, H. M. *et al.* (1994). Role of HLA-A motifs in identification of potential CTL epitopes in human papillomavirus type 16 E6 and E7 proteins. *J. Immunol.* **152**, 3904–3912.

9. Mandelboim, O., Bar-Haim, E., Vadai, E., Fridkin, M. & Eisenbach, L. (1997). Identification of shared tumor-associated antigen peptides between two spontaneous lung carcinomas. *J. Immunol.* **159**, 6030–6036.

10. Daser, A., Urlaub, H. & Henklein, P. (1994). HLA-B27 binding peptides derived from the 57 kD heat shock protein of *Chlamydia trachomatis*: novel insights into the peptide binding rules. *Mol. Immunol.* **31**, 331–336.

11. Gao, L., Walter, J., Travers, P., Stauss, H. & Chain, B. M. (1995). Tumor-associated E6 protein of human papillomavirus type 16 contains an unusual H-2Kb-restricted cytotoxic T cell epitope. *J. Immunol.* **155**, 5519–5526.

12. Apostolopoulos, V., Karanikas, V., Haurum, J. S. & McKenzie, I. F. (1997). Induction of HLA-A2-restricted CTLs to the mucin 1 human breast cancer antigen. *J. Immunol.* **159**, 5211–5218.

13. Apostolopoulos, V., Haurum, J. S. & McKenzie, I. F. (1997). MUC1 peptide epitopes associated with five different H-2 class I molecules. *Eur. J. Immunol.* **27**, 2579–2587.

14. Apostolopoulos, V., Chelvanayagam, G., Xing, P. X. & McKenzie, I. F. (1998). Anti-MUC1 antibodies react directly with MUC1 peptides presented by class I H2 and HLA molecules. *J. Immunol.* **161**, 767–775.

15. Gendler, S. J., Burchell, J. M., Duhig, T., Lamport, D., White, R., Parker, M. *et al.* (1987). Cloning of partial cDNA encoding differentiation and tumor-associated mucin glycoproteins expressed by human mammary epithelium. *Proc. Natl Acad. Sci. USA*, **84**, 6060–6064.

16. Gendler, S. J., Lancaster, C. A., Taylor-Papadimitriou, J., Duhig, T., Peat, N., Burchell, J. *et al.* (1990). Molecular cloning and expression of human tumor-associated polymorphic epithelial mucin. *J. Biol. Chem.* **265**, 15286–15293.

17. Apostolopoulos, V., Pietersz, G. A. & McKenzie, I. F. (1999). MUC1 and breast cancer. *Curr. Opin. Mol. Ther.* **1**, 98–103.

18. Apostolopoulos, V., Pietersz, G. A., Loveland, B. E., Sandrin, M. S. & McKenzie, I. F. (1995). Oxidative/reductive conjugation of mannan to antigen selects for T1 or T2 immune responses. *Proc. Natl Acad. Sci. USA*, **92**, 10128–10132.

19. Apostolopoulos, V., Pietersz, G. A. & McKenzie, I. F. (1996). Cell-mediated immune responses to MUC1 fusion protein coupled to mannan. *Vaccine*, **14**, 930–938.

20. Apostolopoulos, V., Pietersz, G. A. & McKenzie, I. A. (2000). Studies of MUC1 peptides. In *Peptide Based Cancer Vaccines* (Kast, M., ed.), pp. 106–120, Landes Bioscience, Chapman & Hall, London. Chapter 7.

21. Lofthouse, S. A., Apostolopoulos, V., Pietersz, G. A., Li, W. & McKenzie, I. F. (1997). Induction of T1 (cytotoxic lymphocyte) and/or T2 (antibody) responses to a mucin-1 tumour antigen. *Vaccine*, **15**, 1586–1593.

22. Pietersz, G. A., Li, W., Popovski, V., Caruana, J. A., Apostolopoulos, V. & McKenzie, I. F. (1998). Parameters for using mannan–MUC1 fusion protein to induce cellular immunity. *Cancer Immunol. Immunother.* **45**, 321–326.

23. Gillanders, W. E., Hanson, H. L., Rubocki, R. J., Hansen, T. H. & Connolly, J. M. (1997). Class I-restricted cytotoxic T cell recognition of split peptide ligands. *Int. Immunol.* **9**, 81–89.

24. Eisen, H. N., Sykulev, Y. & Tsomides, T. J. (1996). Antigen-specific T-cell receptors and their reactions with complexes formed by peptides with major histocompatibility complex proteins. *Advan. Protein Chem.* **49**, 1–56.

25. Reddehase, M. J., Rothbard, J. B. & Koszinowski, U. H. (1989). A pentapeptide as minimal antigenic determinant for MHC class I-restricted T lymphocytes. *Nature*, **337**, 651–653.

26. Horig, H., Young, A. C., Papadopoulos, N. J., DiLorenzo, T. P. & Nathenson, S. G. (1999). Binding of longer peptides to the H-2K^b heterodimer is restricted to peptides extended at their C terminus: refinement of the inherent MHC class I peptide binding criteria. *J. Immunol.* **163**, 4434–4441.

27. Collins, E. J., Garboczi, D. N. & Wiley, D. C. (1994). Three-dimensional structure of a peptide extending from one end of a class I MHC binding site. *Nature*, **371**, 626–629.

28. Jameson, S. C. & Bevan, M. J. (1992). Dissection of major histocompatibility complex (MHC) and T cell receptor contact residues in a K^b-restricted ovalbumin peptide and an assessment of the predictive power of MHC-binding motifs. *Eur. J. Immunol.* **22**, 2663–2667.

29. Fremont, D. H., Stura, E. A., Matsumura, M., Peterson, P. A. & Wilson, I. A. (1995). Crystal structure of an H-2K^b–ovalbumin peptide complex reveals the interplay of primary and secondary anchor positions in the major histocompatibility complex binding groove. *Proc. Natl Acad. Sci. USA*, **92**, 2479–2483.

30. Guo, H. C., Jardetzky, T. S., Garrett, T. P., Lane, W. S., Strominger, J. L. & Wiley, D. C. (1992). Different length peptides bind to HLA-Aw68 similarly at their ends but bulge out in the middle. *Nature*, **360**, 364–366.

31. Chen, W., McCluskey, J., Rodda, S. & Carbone, F. R. (1993). Changes at peptide residues buried in the major histocompatibility complex (MHC) class I binding cleft influence T cell recognition: a possible role for indirect conformational alterations in the MHC class I or bound peptide in determining T cell recognition. *J. Expt. Med.* **177**, 869–873.

32. Madden, D. R., Garboczi, D. N. & Wiley, D. C. (1993). The antigenic identity of peptide–MHC complexes: a comparison of the conformations of five viral peptides presented by HLA-A2. *Cell*, **75**, 693–708.

33. Garcia, K. C., Degano, M., Pease, L. R., Huang, M., Peterson, P. A., Teyton, L. *et al.* (1998). Structural basis of plasticity in T cell receptor recognition of a self peptide–MHC antigen. *Science*, **279**, 1166–1172.

34. McRee, D. E. (1993). *Practical Protein Crystallography*, Academic Press, San Diego.

35. Eriksson, A. E., Baase, W. A., Zhang, X. J., Heinz, D. W., Blaber, M., Baldwin, E. P. *et al.* (1992). Response of a protein structure to cavity-creating mutations and its relation to the hydrophobic effect. *Science*, **255**, 178–183.

36. Froloff, N., Windemuth, A. & Honig, B. (1997). On the calculation of binding free energies using continuum methods: application to MHC class I protein–peptide interactions. *Protein Sci.* **6**, 1293–1301.

37. Degano, M., Garcia, K. C., Apostolopoulos, V., Rudolph, M. G., Teyton, L. & Wilson, I. A. (2000). A functional hot spot for antigen recognition in a superagonist TCR/MHC complex. *Immunity*, **12**, 251–261.

38. Ding, Y. H., Baker, B. M., Garboczi, D. N., Biddison, W. E. & Wiley, D. C. (1999). Four A6-TCR/peptide/HLA-A2 structures that generate very different T cell signals are nearly identical. *Immunity*, **11**, 45–56.

39. Molano, A., Erdjument-Bromage, H., Fremont, D. H., Messaoudi, I., Tempst, P. & Nikolic-Zugic, J. (1998). Peptide selection by an MHC H-2K^b class I molecule devoid of the central anchor (C) pocket. *J. Immunol.* **160**, 2815–2823.

40. Saito, Y., Peterson, P. A. & Matsumura, M. (1993). Quantitation of peptide anchor residue contributions to class I major histocompatibility complex molecule binding. *J. Biol. Chem.* **268**, 21309–21317.

41. Lawrence, M. C. & Colman, P. M. (1993). Shape complementarity at protein/protein interfaces. *J. Mol. Biol.* **234**, 946–950.

42. Torigoe, H., Nakayama, T., Imazato, M., Shimada, I., Arata, Y. & Sarai, A. (1995). The affinity maturation of anti-4-hydroxy-3-nitrophenylacetyl mouse monoclonal antibody. A calorimetric study of the antigen–antibody interaction. *J. Biol. Chem.* **270**, 22218–22222.

43. Jeffrey, P. D., Strong, R. K., Sieker, L. C., Chang, C. Y., Campbell, R. L., Petsko, G. A. *et al.* (1993). 26–10 Fab–digoxin complex: affinity and specificity due to surface complementarity. *Proc. Natl Acad. Sci. USA*, **90**, 10310–10314.

44. Connolly, J. M. (1983). Analytical molecular surface calculation. *J. Appl. Crystallog.* **16**, 548–558.

45. Rudolph, M. G., Speir, J. A., Brunmark, A., Mattsson, N., Jackson, M. R., Peterson, P. A. *et al.* (2001). The crystal structures of K^{bm1} and K^{bm8} reveal that subtle changes in the peptide environment impact thermostability and alloreactivity. *Immunity*, **14**, 231–242.

46. Khan, A. R., Baker, B. M., Ghosh, P., Biddison, W. E. & Wiley, D. C. (2000). The structure and stability of an HLA-A*0201/octameric tax peptide complex with an empty conserved peptide–N-terminal binding site. *J. Immunol.* **164**, 6398–6405.

47. Glithero, A., Tormo, J., Haurum, J. S., Arsequell, G., Valencia, G., Edwards, J. *et al.* (1999). Crystal structures of two H-2D^b/glycopeptide complexes

suggest a molecular basis for CTL cross-reactivity. *Immunity*, **10**, 63−74.

48. Smith, K. J., Reid, S. W., Harlos, K., McMichael, A. J., Stuart, D. I., Bell, J. I. *et al.* (1996). Bound water structure and polymorphic amino acids act together to allow the binding of different peptides to MHC class I HLA-B53. *Immunity*, **4**, 215−228.

49. Tirosh, B., el-Shami, K., Vaisman, N., Carmon, L., Bar-Haim, E., Vadai, E. *et al.* (1999). Immunogenicity of H-2K^b-low affinity, high affinity, and covalently bound peptides in anti-tumor vaccination. *Immunol. Letters*, **70**, 21−28.

50. Matsumura, M., Saito, Y., Jackson, M. R., Song, E. S. & Peterson, P. A. (1992). *In vitro* peptide binding to soluble empty class I major histocompatibility complex molecules isolated from transfected *Drosophila melanogaster* cells. *J. Biol. Chem.* **267**, 23589−23595.

51. Stura, E. A., Matsumura, M., Fremont, D. H., Saito, Y., Peterson, P. A. & Wilson, I. A. (1992). Crystallization of murine major histocompatibility complex class I H-2K^b with single peptides. *J. Mol. Biol.* **228**, 975−982.

52. Jackson, M. R., Song, E. S., Yang, Y. & Peterson, P. A. (1992). Empty and peptide-containing conformers of class I major histocompatibility complex molecules expressed in *Drosophila melanogaster* cells. *Proc. Natl Acad. Sci. USA*, **89**, 12117−12121.

53. Otwinowski, Z. & Minor, W. (1997). Processing of X-ray diffraction data collected in oscillation mode. *Methods Enzymol.* **276**, 307−326.

54. Navaza, J. (1994). AMoRe: an automated package for molecular replacement. *Acta Crystallog.* **50**, 157−163.

55. Brünger, A. T., Adams, P. D., Clore, G. M., DeLano, W. L., Gros, P., Grosse-Kunstleve, R. W. *et al.* (1998). Crystallography and NMR system: a new software suite for macromolecular structure determination. *Acta Crystallog. sect. D*, **54**, 905−921.

56. Read, R. J. (1986). Improved Fourier coefficients for maps using phases from partial structures with errors. *Acta Crystallog. sect. D*, **42**, 140−159.

57. Jones, T. A., Zou, J. Y., Cowan, S. W. & Kjeldgaard, A. (1991). Improved methods for binding protein models in electron density maps and the location of errors in these models. *Acta Crystallog. sect. A*, **47**, 110−119.

58. Brünger, A. T. (1992). Free R value: a novel statistical quantity for assessing the accuracy of crystal structures. *Nature*, **355**, 472−475.

59. Laskowski, R. A., MacArthur, M. W., Moss, D. & Thornton, J. (1993). PROCHECK: a program to check the stereochemical quality of protein structures. *J. Appl. Crystallog.* **26**, 283−291.

60. Carbone, F. R. & Bevan, M. J. (1989). Induction of ovalbumin-specific cytotoxic T cells by *in vivo* peptide immunization. *J. Expt. Med.* **169**, 603−612.

61. Van Bleek, G. M. & Nathenson, S. G. (1990). Isolation of an endogenously processed immunodominant viral peptide from the class I H-2K^b molecule. *Nature*, **348**, 213−216.

62. Bonneau, R. H., Salvucci, L. A., Johnson, D. C. & Tevethia, S. S. (1993). Epitope specificity of H-2K^b-restricted. HSV-1-, and HSV-2-cross-reactive cytotoxic T lymphocyte clones. *Virology*, **195**, 62−70.

63. Tallquist, M. D., Yun, T. J. & Pease, L. R. (1996). A single T cell receptor recognizes structurally distinct MHC/peptide complexes with high specificity. *J. Expt. Med.* **184**, 1017−1026.

64. Udaka, K., Wiesmuller, K. H., Kienle, S., Jung, G. & Walden, P. (1996). Self-MHC-restricted peptides recognized by an alloreactive T lymphocyte clone. *J. Immunol.* **157**, 670−678.

65. Sykulev, Y., Vugmeyster, Y., Brunmark, A., Ploegh, H. L. & Eisen, H. N. (1998). Peptide antagonism and T cell receptor interactions with peptide−MHC complexes. *Immunity*, **9**, 475−483.

66. Kast, W. M., Roux, L., Curren, J., Blom, H. J., Voordouw, A. C., Meloen, R. H. *et al.* (1991). Protection against lethal Sendai virus infection by *in vivo* priming of virus-specific cytotoxic T lymphocytes with a free synthetic peptide. *Proc. Natl Acad. Sci. USA*, **88**, 2283−2287.

67. Franco, M. A., Lefevre, P., Willems, P., Tosser, G., Lintermanns, P. & Cohen, J. (1994). Identification of cytotoxic T cell epitopes on the VP3 and VP6 rotavirus proteins. *J. Gen. Virol.* **75**, 589−596.

68. Laskowski, R. A. (1995). SURFNET: a program for visualizing molecular surfaces, cavities and intermolecular interactions. *J. Mol. Graph.* **13**, 323−330.

69. Nicholls, A., Sharp, K. A. & Honig, B. (1991). Protein folding and association: insights from the interfacial and thermodynamic properties of hydrocarbons. *Proteins: Struct. Funct. Genet.* **11**, 281−296.

Edited by D. Rees